In Situ Stress and Nanogravimetric Measurements during Underpotential Deposition of Bismuth on (111)-Textured Au

G. R. Stafford* and U. Bertocci

Materials Science and Engineering Laboratory, National Institute of Standards and Technology, Gaithersburg, Maryland 20899

Received: May 2, 2006; In Final Form: June 16, 2006

The surface stress associated with the underpotential deposition (upd) of bismuth on (111)-textured Au is examined, using the wafer curvature method, in acidic perchlorate and nitrate supporting electrolyte. The surface stress is correlated to Bi coverage by independent nanogravimetric measurements using an electrochemical quartz crystal nanobalance. The mass increase measured in the presence of perchlorate is consistent with the (2×2) and $(p \times \sqrt{3})$-2Bi adlayers reported in the literature. ClO_4^- does not play a significant role in the upd process. The complete Bi monolayer causes an overall surface stress change of about -1.4 N m^{-1}. We attribute this compressive stress to the formation of Bi−Au bonds which partially satisfy the bonding requirements of the Au surface atoms, thereby reducing the tensile surface stress inherent to the clean Au surface. At higher Bi coverage, an additional contribution to the compressive stress is due to the electrocompression of the $(p \times \sqrt{3})$-2Bi adlayer. In nitric acid electrolyte, NO_3^- coadsorbs with Bi over the entire upd region but has little fundamental impact on adlayer structure and stress.

Introduction

Bismuth has become an interesting topic for the electrochemical community in recent years due to its unique electrical, physical, and chemical properties. Bismuth thin films have demonstrated large magnetoresistance,[1] thermoelectric efficiency,[2] and desirable quantum effects.[3] An electrochromic system based on the reversible electrodeposition of bismuth has shown promise for electrochemical device applications.[4,5] Bismuth deposition has also been examined on semiconductor substrates.[6,7] Submonolayers of bismuth on some noble metal surfaces have shown enhanced catalytic activity for a variety of electroreduction processes, most notably the two-electron reduction of H_2O_2 to H_2O, often the limiting step in the reduction of O_2 to H_2O in aqueous fuel cells.[8,9] For this reason the underpotential deposition (upd) of bismuth on a variety of noble metal substrates has been extensively examined by in situ techniques such as electrochemical voltammetry/coulometry,[8,10−16] scanning probe microscopy,[9,17−19] X-ray scattering,[17,20] quartz crystal nanogravimetry,[21] impedance spectroscopy,[22,23] spectral reflectance spectroscopy,[24,25] and surface conductivity,[26] in order to better understand the relationship between the structure of the upd adlayers and the electrocatalytic activity.

The upd region of Bi on Au(111) shows several interesting structural features. At about 0.25 V positive of the bulk deposition potential, Bi forms a (2×2) structure, commensurate with the underlying Au surface.[9,13,17,18,20] Open structures of this type are unique to electrochemical processing and there is some debate as to whether these low-coverage adlayers are stabilized by the coadsorption of anions or are the result of Coulombic repulsion due to a partial charge remaining on the Bi adatom. Electrosorption valencies ranging from 2.6 to 3 have been reported for this system in the upd region.[13,21,24] As the potential is made more negative and the Bi coverage increases, the (2×2) structure is replaced by a uniaxially commensurate $(p \times \sqrt{3})$-2Bi adlayer.[9,13,17,18,20] This structure can be electrocompressed in the incommensurate direction with areal coverage varying with potential from 61% to 67%.[17] When the reversible potential for Bi is reached, the bulk deposition of Bi proceeds on this compressed $(p \times \sqrt{3})$-2Bi adlayer. For this reason, an understanding of Bi deposition in the upd region may help us better understand the growth and subsequent properties of bulk thin films.

An additional in situ probe gaining popularity in electrochemistry involves the measurement of surface and growth stress. Several techniques have been developed, most of which are outlined in a series of review papers by Weil.[27−29] The simplest and most widely used methods involve the measurement of the deflection of a flexible cathode, typically in a direction that is perpendicular to the in-plane stress generated in the film. Fairly sophisticated methods for tracking this deflection have been developed in the last 20 years. The more popular make use of interferometry,[30,31] capacitance measurements,[32] laser beam reflection,[33−37] and scanning tunneling microscopy/atomic force microscopy.[38−40]

Surface stress is the reversible work required to elastically deform a surface. The loss of bonds at a clean metal surface causes an increased charge density between the remaining surface atoms, thereby increasing their attractive interaction and resulting in a tensile stress at the surface. The adsorption of species on the surface can also be expected to alter the surface stress, since the local interaction of each adsorbate will alter the bond strength between neighboring atoms on the surface. This holds as long as the adsorbate changes the density of the binding electrons, which is realistic for free-electron and transition metals. Excellent reviews of the subject have appeared in the literature.[41,42]

Surface stress can also be generated as the result of the lattice misfit between a metal adlayer and the substrate. The sensitivity of surface stress to both ionic and fully discharged adsorbates makes this measurement particularly relevant for upd studies where both processes tend to occur simultaneously.[38,43,44] For

10.1021/jp062689l
Published on Web 07/19/2006

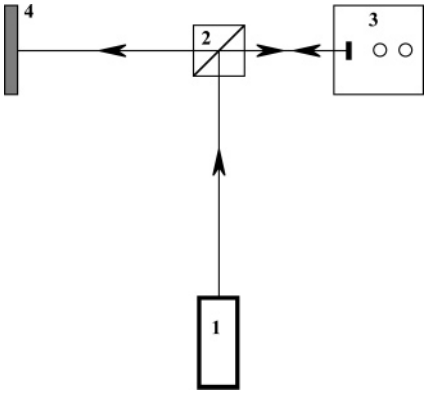

Figure 1. The laser path: 1, He−Ne laser; 2, beam splitter; 3, electrochemical cell; 4, position-sensitive detector.

example, both Brunt and Seo have examined the surface stress changes associated with the upd of Pb on Au(111) and observed a relaxation in the compressive stress of the incommensurate adlayer in the potential region where the rotational angle of the monolayer changes from 0° to 2.5°.[45,46] The compressive stress generated as the result of electrocompression also compared favorably to that expected from the reported strain.[45,47]

In this paper, we examine the surface stress associated with the upd of Bi onto (111)-textured Au cantilever electrodes from both perchloric acid and nitric acid electrolyte. To correlate the stress development with the Bi coverage, we separately examine the process using an electrochemical quartz crystal nanobalance (EQNB).

Experimental Section

A schematic of the components of the in situ stress measurement apparatus is shown in Figure 1. The light source was a 1 mW helium−neon laser (JDS Uniphase, model 1108P). (Certain trade names are mentioned for experimental information only, in no case does it imply a recommendation or endorsement by NIST.) A beam splitter (50% reflected, 50% transmitted) was placed in the path of the beam to direct the laser to the back of the cantilever working electrode and yet allow the beam reflected from the cantilever to reach the position sensitive detector (PSD). The incident and reflected beams were initially coincident. A duo-lateral PSD with dimensions 20 mm × 20 mm (DLS-20 from UTD Sensors Inc.) was used to measure the position of the reflected beam. The four photocurrents from the PSD were amplified, measured by a National Instrument A/D card, and transferred to a Macintosh Power PC computer. The signals were converted into vertical and horizontal positions on the PSD. The stress calculation utilized only the vertical position of the laser.

The cantilever was a borosilicate glass slide (D 263, Schott) measuring 60 mm × 3 mm × 0.108 mm. The glass had a Young's modulus of 72.9×10^9 N m^{-2} and a Poisson ratio of 0.208, as specified by the vendor. Onto one side of this substrate a 4 nm thick adhesion layer of titanium and a 250 nm film of gold were vapor deposited by electron-beam evaporation. The glass−metal interface provided the reflective surface for the laser beam. Prior to use, the electrodes were cleaned in piranha solution (3:1 volume mixture of H_2SO_4:H_2O_2). The Au electrodes had a strong (111) crystallographic orientation. The 200 reflection was not apparent in $\theta-2\theta$ X-ray scans and rocking curves of the 111 reflection generally yielded a full-width half-maximum (fwhm) on the order of 2°.

Two electrolytes were examined: 10 mmol L^{-1} Bi_2O_3 (J.T. Baker) in 1.0 mol L^{-1} $HClO_4$ (Sigma-Aldrich, 99.999%) and 0.10 mol L^{-1} $Bi(NO_3)_3$ (Sigma-Aldrich, 99.999%) in 1.0 mol L^{-1} HNO_3 (Alfa Aesar, Environmental Grade Plus). The distilled water was further purified using an EASY pure UV ultrapure water system (Barnstead). The electrochemical cell was a single-compartment Pyrex cell covered by a perfluorethylene cap. A glass disk was joined to the back of the cell to allow the cell to be held and positioned by a standard mirror mount on the optical bench. The counter electrode was platinum foil placed parallel to and in the same solution as the working electrode. The reference electrode was a saturated Hg sulfate electrode (SSE) that was separated from the working compartment by a Vycor-tipped bridge filled with either 1 mol L^{-1} HNO_3 or 1.0 mol L^{-1} $HClO_4$, depending on the working electrolyte. The potentials reported are with respect to the bulk deposition of Bi, which in this electrolyte occurs at −0.465 V/SSE. Prior to making a measurement, the electrolyte was purged with nitrogen. A nitrogen purge above the electrolyte was continued during a measurement. Potential control was maintained using an EG&G Princeton Applied Research Corp. (PARC) model 273 potentiostat/galvanostat that was controlled by a Macintosh Power PC computer and LabView software.

We examined the changes in surface stress of the Au cantilever in response to changes in surface chemistry in the upd region for bismuth on gold. Since the Au electrode is on the side away from the laser, compressive stress displaces the cantilever toward the laser while tensile stress displaces the cantilever away from the laser. The relationship between the surface stress and the radius of curvature of the cantilever is given by Stoney's equation[48]

$$\tau^{(s)} = \frac{E_s t_s^{\,2}}{6(1-\nu_s)R} \tag{1}$$

where E_s, ν_s, and t_s are Young's modulus, Poisson ratio, and thickness of the glass substrate, respectively, and R is the radius of curvature of the cantilever. Equation 2 is Stoney's equation in terms of the PSD output

$$\tau^{(s)} = \frac{E_s t_s^{\,2} n_{air} d_{psd}}{6(1-\nu_s)2Ln_{el}D_{psd}} \tag{2}$$

where d_{psd} is the vertical coordinate of the reflected laser beam onto the PSD, D_{psd} is the distance of the PSD from the electrode, and L is the length of electrode submerged into the electrolyte down to where the laser strikes the electrode. Since the electrochemical cell is filled with electrolyte, a correction must be made to account for the difference in the refractive index between the electrolyte inside the cell ($n_{el} = 1.33$) and the air outside the cell ($n_{air} = 1.0$). During a measurement $\tau^{(s)}$ is determined from d_{psd} using eq 2. In the configuration used for these experiments, this apparatus can resolve surface stresses on the order of 10^{-3} N m^{-1}. A more detailed description of the optical bench and stress measurement can be found in ref 49.

Mass changes during Bi upd were monitored by means of the EQNB. The measuring apparatus was a RQCM from Maxtek, Inc., also the manufacturer of the quartz crystals used. They were polished 2.54 cm AT cut blanks, onto which first Ti and then Au was evaporated. Their resonance frequency was 5 MHz. The Au deposit had a strong (111) crystallographic orientation, and rocking curves of the 111 reflection generally yielded a fwhm on the order of 3°. The EQNB as well as the EG&G 273 potentiostat−galvanostat were driven by Labview software on a Macintosh Power PC computer.

The cell in which the Au-covered quartz crystal was the working electrode had a separated compartment for the counter

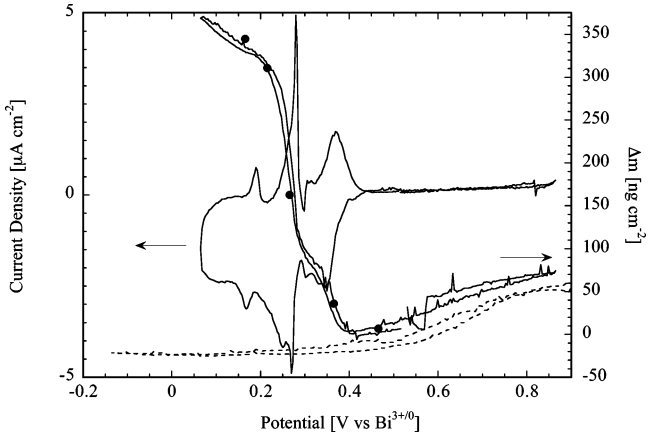

Figure 2. Potentiodynamic scan and mass changes on (111)-textured Au in 1.0 mol/L $HClO_4$ (dashed line) and 10 mmol/L Bi_2O_3 + 1.0 mol/L $HClO_4$ (solid line). Sweep rate = 1 mV/s. Solid points are mass changes obtained potentiostatically.

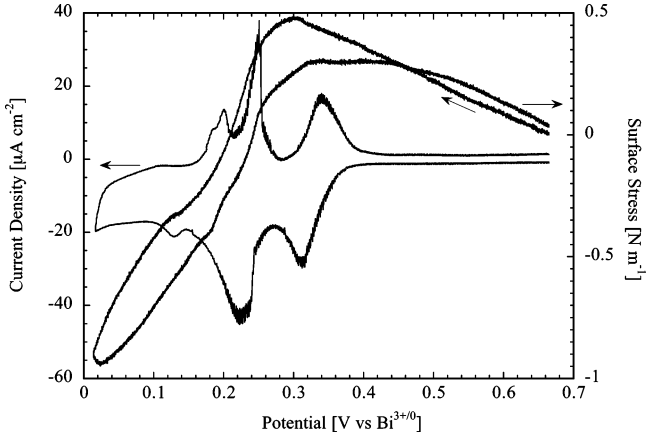

Figure 3. Potentiodynamic scan (10 mV/s) and surface stress on (111)-textured Au in 10 mmol/L Bi_2O_3 + 1.0 mol/L $HClO_4$.

electrode and a SSE reference electrode connected via a Luggin−Haber capillary. The cell had a magnetic stirrer, and N_2 could be bubbled in the main compartment to speed up deaeration or could flow above the solution, maintaining a small overpressure inside the cell. Most measurements consisted of potentiodynamic sweeps, but occasionally, potentiostatic or galvanostatic measurements were performed. The Maxtek, Inc., RQCM measures both the resonant frequency and the resistance R_1 of the equivalent resonant circuit: R_1 in all upd measurements changed very little, confirming that no significant roughening of the electrode surface took place. EQNB measurements in the pure acids were also carried out, to determine the voltage range where anion adsorption and desorption occurred.

Results

Perchloric Acid. Figure 2 shows both the voltammetric and gravimetric response of the Au-covered quartz electrode for the Bi upd region in both 1 mol L^{-1} $HClO_4$ and 1 mol L^{-1} $HClO_4$ containing 10 mmol L^{-1} Bi^{3+}. In addition to the potentiodynamic curves, gravimetric results from stepwise potentiostatic measurements are shown. The agreement is excellent. Potentiodynamic scans at different sweep rates (1−100 mV s^{-1}) have also been performed, with practically identical results. Anion desorption is the dominant feature as the potential approaches 0.40 V from more positive values. The gravimetric response in the absence of Bi^{3+} shows that ClO_4^- desorption is essentially complete prior to Bi upd. Since the potential of zero charge (pzc) for Au(111) in 1.0 mol L^{-1} $HClO_4$ is +0.38 V/$Bi^{3+/0}$,[50] perchlorate desorption is expected in this potential range. Bismuth upd occurs in three steps that were identified by changes in slope of the gravimetric curve. These steps roughly correspond to the current peaks in the voltammetry. The location of these voltammetric peaks is very similar to that reported by others in $HClO_4$.[8,13,21] In the first gravimetric step, from 0.40 to 0.27 V, the mass gain Δm is about 90 ± 10 ng cm^{-2}. In the second step, from 0.27 to 0.20 V, Δm is 250 ± 50 ng cm^{-2}, while the third step which approaches bulk bismuth deposition, entails an additional Δm of 90 ± 10 ng cm^{-2}.

The roughness factor of the Au-covered quartz electrode was determined by carrying out potentiodynamic sweeps up to 1.50 V/$Bi^{3+/0}$ and measuring the charge necessary for the complete reduction of the Au oxide. A charge of 560 ± 20 μC cm^{-2} was measured in perchloric acid. Since the theoretical value for Au(111) is 222 μC cm^{-2} per electron, assuming that one oxygen is adsorbed for each surface atom of Au,[51] the roughness factor is calculated to be 1.3. On this basis it is possible to estimate the degree of Bi coverage after the first and second gravimetric step, as well as immediately prior to bulk deposition. After the first step, about 0.14 monolayers (ML) of Bi is deposited, with respect to the Au(111) surface. This means that the (2 × 2)-Bi structure is not fully formed after the first gravimetric step. After the second step, about 0.54 ML is formed, somewhat less than the 0.61 ML associated with the uncompressed ($p \times \sqrt{3}$)-2Bi adlayer. Immediately prior to bulk Bi deposition, the Bi adlayer is about 0.72 ML, which is consistent with the 0.67 ML coverage reported for the fully compressed ($p \times \sqrt{3}$)-2Bi structure.[17,52]

Scanning probe and X-ray scattering measurements have shown that the (2 × 2)-Bi structure is stable in the potential range of +0.19 to +0.28 V/$Bi^{3+/0}$,[13,17,18,20] which places it well into the second voltammetric peak that is centered at +0.26 V/$Bi^{3+/0}$. The broad peak centered at +0.35 V/$Bi^{3+/0}$ has been attributed to a disordered adlayer[20] as well as a variety of one-dimensional phases, i.e., decoration of steps and defects, which appear in relatively high quantity.[14] Our gravimetric results in perchlorate indicate that the (2 × 2)-Bi structure is not fully formed after the completion of the first voltammetric peak. The data also suggest that the ($p \times \sqrt{3}$)-2Bi structure begins to form prior to the completion of the second voltammetric peak but is not fully formed at the completion of the second voltammetric peak. The electrocompression region, where the Bi adlayer uniaxially compresses along the incommensurate direction, resulting in a coverage increase from 0.61 to 0.67 ML, is well-supported by our data. The fact that our measured mass increases are generally consistent with the reported coverages for the various Bi adlayers suggests that ClO_4^- does not play a significant role in the upd process.

The surface stress response for Bi upd is shown in Figure 3 and consists of three distinct features. In the potential range of +0.65 to +0.30 V/$Bi^{3+/0}$ the surface stress moves in the tensile (positive) direction from a value arbitrarily chosen as zero. The stress response reflects the desorption of ClO_4^- from the gold surface. This is consistent with Ibach's surface-induced charge redistribution model where electron acceptors such as adsorbed anions cause compressive stress since they reduce the electron density in the surface.[32] As the potential approaches the pzc from the positive direction, ClO_4^- is desorbed and its compressive contribution to the surface stress is diminished. Haiss has observed a linear correlation between surface stress and surface charge for a variety of anions on Au.[53]

In the potential range of +0.30 to +0.20 V/$Bi^{3+/0}$, where the (2 × 2)-Bi adlayer is formed, the surface stress moves in the compressive direction. It is interesting to note that the stress

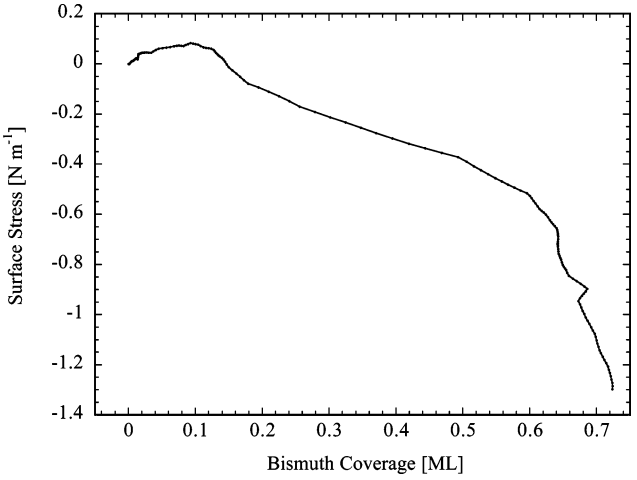

Figure 4. Surface stress as a function of Bi coverage in monolayers on (111)-textured Au in 10 mmol/L Bi_2O_3 + 1.0 mol/L $HClO_4$.

maximum occurs well into the upd region, near the completion of the first voltammetric peak. At more negative potentials where the adlayer transforms to the ($p \times \sqrt{3}$)-2Bi structure, the stress continues in the compressive direction although the slope, with respect to the potential, decreases somewhat. When the potential scan is reversed, the stress response of the return sweep follows a path similar to that of the forward scan, although some hysteresis is present. The overall upd process is quite reversible and our results are consistent with reports in the literature that no alloy formation between Au and Bi is observed.[8,10,11,22]

Figure 4 summarizes the gravimetric and surface stress response for Bi adlayer formation in $HClO_4$ where the gravimetric data are converted from mass to monolayer coverage with respect to the Au(111) surface. The surface stress was arbitrarily set to zero at the potential where the mass increase begins at about 0.4 V. At very low coverage, the surface stress moves in the tensile direction before becoming compressive for the remainder of adlayer formation. At intermediate coverage, the stress change is essentially linear and then increases rather significantly at a coverage of 0.6 ML. Interestingly, this corresponds to the coverage where electrocompression is reported to begin.[17] The complete bismuth adlayer causes an overall stress change of about -1.4 N m^{-1} with respect to the maximum at 0.1 ML.

There are several possible contributions to the compressive stress generated during Bi adlayer formation. The first involves the Bi−Au bond and its impact on the surface stress of the Au. Experiments[54,55] as well as semiemprical[56] and first-principles[57] calculations indicate that the clean Au(111) surface has a tensile stress of about 2 N m^{-1}. As mentioned previously, this is due to the increased charge density between the surface atoms due to loss of bonding partners. The Au−Bi bond is fairly strong, of the order of 290 kJ mol^{-1}. The addition of Bi to the surface partially satisfies the bonding requirements of the Au surface atoms, decreasing the charge density and reducing the tensile surface stress. One would expect that in the absence of Bi−Bi interactions, the adlayer-induced surface stress would increase linearly with coverage.[41]

As the Bi coverage increases, stresses within the adlayer can contribute to cantilever deflection. Attempts to quantify the stress associated with heteroepitaxial metal on metal growth using continuum elasticity theory and using the difference between the bulk lattice parameters to determine a misfit strain yield mixed results.[58] When the misfit is positive (small adsorbate), elasticity theory predicts a tensile stress, yet there are several examples where the opposite is true, namely, Cu on Au(111).[39,49] However, elasticity theory is in fairly good agreement with experimental observations in predicting the level of compressive stress when the misfit is negative (large adsorbate).[58] From the misfit of the lattice constants, one can calculate the stress that arises from the elastic deformation of the deposit when it grows pseudomorphically on the substrate

$$\tau^{(s)} = Y'_{(111)}\epsilon_{mf}d_{(111)}\Theta \tag{3}$$

where $Y'_{(111)}$ is the biaxial modulus of the adsorbate (111) surface, $d_{(111)}$ is the thickness of one monolayer, ϵ_{mf} is the misfit, and Θ is the coverage in monolayers. Since Bi does not grow pseudomorphically on Au when the coverage exceeds 25%, we can only use eq 3 as an upper bound for the stress in the Bi adlayer. Bismuth has a rhombohedral crystal structure which means that it does not have a naturally occurring close-packed (111) surface. For this reason we will use the polycrystalline biaxial modulus of 47.7×10^9 N m^{-2}. Assuming an atomic radius for Bi of 0.17 nm, which results in a misfit of -0.18, a $d_{(111)}$ of 0.34 nm, and a coverage of 0.67 ML (for the ($p \times \sqrt{3}$)-2Bi adlayer), eq 3 gives a surface stress of -1.95 N m^{-1}. Since the ($p \times \sqrt{3}$)-2Bi adlayer is uniaxially incommensurate, one would expect it to have a significantly lower stress from that of a pseudomorphic layer of equal coverage.

The elastic contribution of electrocompression of the Bi adlayer to the compressive stress can also be estimated. In the potential range of 0.19−0.01 V/Bi$^{3+/0}$, the Bi atomic distance in the incommensurate direction decreases from 0.471 to 0.447 nm,[17] which decreases the Bi nearest neighbor distance from 0.342 to 0.334 nm. If we apply Hooke's law, treating the Bi monolayer as a free-standing elastic film, then the stress−strain relationship is given by

$$\sigma = -\epsilon Y' d \tag{4}$$

where Y' is the biaxial modulus and d is the film thickness.[59] Using the change in the Bi spacing reported by Chen,[17] we can calculate a strain of 0.023. With the polycrystalline modulus and monolayer thickness used above, eq 4 gives a stress value of -0.37 N m^{-1}. This value is about half of that observed in the electrocompression region (0.6−0.7 ML) in Figure 4.

It is interesting to note that the stress response for Bi on (111)-textured Au is nearly identical in shape and somewhat higher in magnitude than that reported for Pb on Au(111) in $HClO_4$.[45,46] On the basis of the discussion above, the stress response for Pb and Bi on Au(111) should be similar. The Au−Pb bond being energetically favorable (130 kJ mol^{-1}) should decrease the charge density on the Au and induce a compressive stress. In addition, Pb will add an elastic contribution to the compressive stress since it forms a close-packed incommensurate adlayer which also undergoes an electrocompression strain of 0.02. Similar to Bi on Au, the Pb adlayer can be expected to generate a compressive stress.

This raises an interesting point in regards to stress development in upd-generated monolayers. We have discussed two contributions to the stress. The first involves the formation of metallic bonds and its impact on the charge density and surface stress of the substrate. Since upd is at least partially driven by the free energy of dissimilar bonding, one would always expect this contribution to be negative, i.e., generate compressive stress. The second contribution involves the elastic state of the adlayer. This can be either positive or negative, depending on the adlayer structure and lattice misfit. If the adlayer is pseudomorphic with the substrate and the misfit is negative (large adsorbate), both

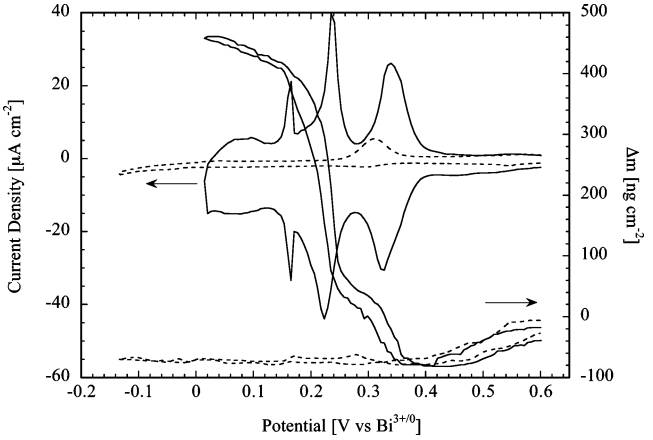

Figure 5. Potentiodynamic scan and mass changes on (111)-textured Au in 1 mol/L HNO_3 (dashed line) and 0.1 mol/L $Bi(NO_3)_3$ + 1 mol/L HNO_3 (solid line). Sweep rate = 10 mV/s.

contributions will be negative and the stress will be compressive. However, when the misfit is positive (small adsorbate), then the sign of the stress depends on the relative contributions of the bonding and the elastic components. In the case of Cu on Au(111), the Cu−Au bond strength (235 kJ mol^{-1}) makes a larger contribution than the +11.4% misfit and a compressive stress is generated.[39,49]

Nitric Acid. Figure 5 shows voltammetry and EQNB data for 1.0 mol L^{-1} HNO_3 with and without Bi^{3+} in solution. The Bi-free background data show that anion desorption is essentially complete prior to Bi upd. Since the pzc for Au(111) in 1.0 mol L^{-1} HNO_3 is +0.3 V/$Bi^{3+/0}$, nitrate desorption is expected in this potential range.[14] The voltammetry in pure acid also shows a small anodic peak at +0.3 V; however there is no mass change associated with this peak, suggesting that it is not associated with nitrate adsorption. When Bi^{3+} is present, location of the voltammetric peaks is very similar to that reported previously in HNO_3 electrolyte.[14] Qualitatively, the upd results in nitrate are similar to those in perchlorate; however the three gravimetric steps tend to have greater mass. The values are 140 ± 15, 280 ± 40, and 90 ± 10 ng cm^{-2}, respectively. Taking into account a roughness factor of 1.3 for the Au electrode, the mass changes converted to monolayer equivalents are 0.22, 0.67, and 0.81 ML of Bi, respectively. A possible explanation for the difference between perchlorate and nitrate is that, due to a negative shifting of the pzc, the more strongly adsorbed nitrate ion is readsorbed onto the Bi adlayer, similar to that which has been reported for sulfate on upd Cu.[39,44,49]

The surface stress response for Bi upd in 1.0 mol L^{-1} HNO_3 is shown in Figure 6. The stress response is very similar to that observed in $HClO_4$ where a stress maximum separates the anion desorption region from Bi adlayer formation. As in perchlorate, the stress maximum occurs well into the upd region, near the completion of the first voltammetric peak. The full Bi monolayer results in a compressive surface stress of about 1.7 N m^{-1}. The stress response of the return sweep follows a path similar to that of the forward scan, again with some hysteresis present.

Figure 7 summarizes the gravimetric and surface stress response for Bi upd in both $HClO_4$ and HNO_3. Although the shapes of the curves are similar, there are significant differences that can be attributed to the presence of NO_3^-. Since Bi has a more negative pzc than Au, one might expect NO_3^- to readsorb on the fully formed Bi monolayer. However it is clear from the gravimetric transients that nitrate coadsorbs with Bi during the entire upd process. The additional mass that we attribute to nitrate represents less than a monolayer throughout the Bi upd

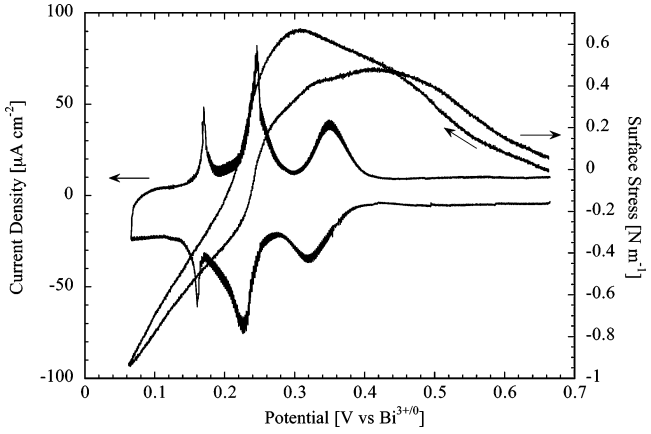

Figure 6. Potentiodynamic scan (10 mV/s) and surface stress on (111)-textured Au in 0.1 mol/L $Bi(NO_3)_3$ + 1 mol/L HNO_3.

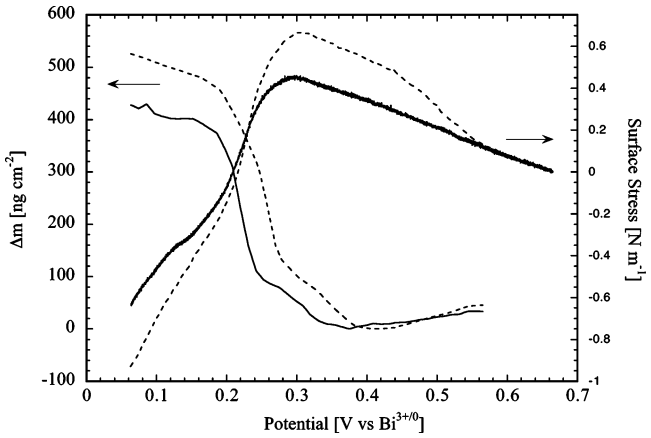

Figure 7. Mass change and surface stress on (111)-textured Au in 10 mmol/L Bi_2O_3 + 1.0 mol/L $HClO_4$ (solid lines) and 0.1 mol/L $Bi(NO_3)_3$ + 1 mol/L HNO_3 (dashed lines).

region. The presence of NO_3^- also alters the stress transient. Nitrate causes a larger tensile stress when it desorbs from the Au surface and a larger compressive stress when it readsorbs onto the Bi surface. These results are consistent with adsorbate-induced stress behavior reported in the literature.[41,42]

Conclusions

We present a gravimetric and surface stress examination of Bi upd on (111)-textured Au in acidic perchlorate and nitrate supporting electrolyte. The complete Bi monolayer causes an overall surface stress change of about −1.4 N m^{-1}. We attribute this compressive stress to two factors: (1) the formation of Bi−Au bonds which partially satisfy the bonding requirements of the Au surface atoms, decreasing the charge density and reducing the tensile surface stress inherent to the clean Au surface; (2) electrocompression of the ($p \times \sqrt{3}$)-2Bi adlayer in the incommensurate direction. ClO_4^- does not play a significant role in the upd process, whereas NO_3^- coadsorbs with Bi over the entire upd region but has little fundamental impact on adlayer structure and stress.

Acknowledgment. The authors gratefully acknowledge the technical contributions of Jonathon Guyer and Carlos Beauchamp.

References and Notes

(1) Jiang, S.; Huang, Y. H.; Luo, F.; Du, N.; Yan, C. H. *Inorg. Chem. Commun.* **2003**, *6*, 781.

(2) Li, L.; Zhang, Y.; Li, G.; Zhang, L. *Chem. Phys. Lett*. **2003**, *378*, 244.
(3) Lu, M.; Zieve, R. J.; van Hulst, A.; Jaeger, H. M.; Rosenbaum, T. F.; Radelaar, S. *Phys. Rev. B* **1996**, *53*, 1609.
(4) Ziegler, J. P. *Solar Energy Mater*. **1999**, *56*, 477.
(5) deTorresi, S. I. C..; Carlos, I. A. *J. Electroanal. Chem*. **1996**, *414*, 11.
(6) Vereecken, P. M.; Rodbell, K.; Ji, C. X.; Searson, P. C. *Appl. Phys. Lett*. **2005**, *86*, 121916.
(7) Vereecken, P. M.; Searson, P. C. *J. Electrochem. Soc.* **2001**, *148*, C733.
(8) Sayed, S.; Juttner, K. *Electrochm. Acta* **1983**, *28*, 1635.
(9) Chen, C.-H.; Gewirth, A. *J. Am. Chem. Soc*. **1992**, 114, 5439.
(10) Schmidt, E.; Gygax, H. R.; Cramer, Y. *Helv. Chim. Acta* **1970**, *53*, 649.
(11) Cadle, S. H.; Bruckenstein, S. J. *J. Electrochem. Soc*. **1972**, *119*, 1166.
(12) Salie, G.; Bartels, K. *Electrochm. Acta* **1994**, *39*, 1057.
(13) Niece, B. K.; Gewirth, A. A. *Langmuir* **1996**, *12*, 4909.
(14) Solomun, T.; Kautek, W. *Electrochim. Acta* **2001**, *47*, 679.
(15) Schultze, J. W.; Dickertmann, D. *Surf. Sci*. **1976**, *54*, 489.
(16) Ganon, J. P.; Clavilier, J. *Surf. Sci.* **1984**, *145*, 487.
(17) Chen, C.-H.; Kepler, K. D.; Gewirth, A. A.; Ocko, B. M.; Wang, J. *J. Phys. Chem.* **1993**, *97*, 7290.
(18) Jeffrey, C. A.; Harrington, D. A.; Morin, S. *Surf. Sci.* **2002**, *512*, L367.
(19) Hara, M.; Nagahara, Y.; Inukai, J.; Yoshimoto, S.; Itaya, K. *Electrochim. Acta* **2006**, *51*, 2327.
(20) Tamura, K.; Wang, J.; Adzic, R.; Ocko, B. *J. Phys. Chem. B* **2004**, *108*, 1992.
(21) Deakin, M. R.; Melroy, O. R. *J. Electroanal. Chem*. **1988**, *239*, 321.
(22) Garland, J.; Assiongbon, K.; Pettit, C.; Emery, S.; Roy, D. *Electrochm. Acta* **2002**, *47*, 4113.
(23) Ragoisha, G. A.; Bondarenko, A. S. *Electrochim. Acta* **2005**, *50*, 1553.
(24) Adzic, R.; Jovancicevic, V.; Podlavicky, M. *Electrochim. Acta* **1980**, *25*, 1143.
(25) Takamura, K.; Watanabe, F.; Takamura, T. *Electrochim. Acta* **1981**, *26*, 979.
(26) Romeo, F. M.; Tucceri, R. I.; Posadas, D. *Surf. Sci*. **1988**, *203*, 186.
(27) Weil, R. *Plating* **1970**, *57*, 1231.
(28) Weil, R. *Plating* **1971**, *58*, 50.
(29) Weil, R. *Plating* **1971**, *58*, 137.
(30) Butler, M. A.; Ginley, D. S. *J. Electrochem. Soc*. **1987**, *134*, 510.
(31) Jaeckel, L.; Lang, G.; Heusler, K. E. *Electrochim. Acta* **1994**, *39*, 1031.
(32) Ibach, H. *J. Vac. Sci. Technol*. **1994**, *A12*, 2240.
(33) Lang, G. G.; Seo, M. *J. Electroanal. Chem*. **2000**, *490*, 98.
(34) Rosolen, J. M.; Decker, F. *J. Electrochem. Soc.* **1996**, *143*, 2417.
(35) Scarminio, J.; Sahu, S. N.; Decker, F. *J. Phys. E, Instrum.* **1989**, *22*, 755.
(36) Chung, K. Y.; Kim, K.-B. *J. Electrochem. Soc*. **200**, *149*, A792.
(37) Seo, M.; Serizawa, Y. *J. Electrochem. Soc.* **2003**, *150* (10), E472.
(38) Brunt, T. A.; Chabala, E. D.; Rayment, T.; O'shea, S. J.; Welland, M. E. *J. Chem. Soc., Faraday Trans*. **1996**, *92*, 3807.
(39) Haiss, W.; Sass, J. K. *J. Electroanal. Chem*. **1995**, *386*, 267.
(40) Raiteri, R.; Butt, H.-J. *J. Phys. Chem*. **1995**, *99*, 15728.
(41) Ibach, H. *Surf. Sci. Rep.* **1997**, *29*, 193.
(42) Haiss, W. *Rep. Prog. Phys.* **2001**, *64*, 591.
(43) Haiss, W.; Sass, J. K. *Langmuir* **1996**, *12*(18), 4311.
(44) Trimble, T.; Tang, L.; Vasiljevic, N.; Dimitrov, N.; van Schilfgaarde, M.; Friesen, C.; Thompson, C. V.; Seel, S. C.; Floro, J. A.; Sieradzki, K. *Phys. Rev. Lett.* **2005**, *95*, 166106.
(45) Brunt, T. A.; Rayment, T.; O'Shea, S. J.; Welland, M. E. *Langmuir* **1996**, *12*, 5942.
(46) Seo, M.; Yamazaki, M. J. *Electrochem. Soc.* **2004**, *151* (8), E276.
(47) Toney, M. F.; Gordon, J. G.; Samant, M. G.; Borges, G. L.; Melroy, O. R.; Yee, D.; Sorenson, L. B. *J. Phys. Chem*. **1995**, *99*, 4733.
(48) Stoney, G. G. *Proc. R. Soc. London, Ser. A* **1909**, *82*, 172.
(49) Kongstein, O. E.; Bertocci, U.; Stafford, G. R. *J. Electrochem. Soc*. **2005**, *152*, C116.
(50) Lecoeur, J.; Rousset, S. *J. Electroanal. Chem*. **2002**, *519*, 18.
(51) Trasatti, S.; Petrii, O. A. *Pure Appl. Chem*. **1991**, *63*, 711.
(52) Tamura, K.; Ocko, B. M.; Wang, J.; Adzic, R. R. *J. Phys. Chem. B* **2002**, *106*, 3896.
(53) Haiss, W.; Nichols, R. J.; Sass, J. K.; Charle, K. P. *J. Electroanal. Chem.* **1998**, *452*, 199.
(54) Tyson, R. W.; Miller, W. A. *Surf. Sci*. **1977**, *62*, 267.
(55) Mays, C. W.; Vermaak, J. S.; Kuhlmann-Wilsdorf, D. *Surf. Sci*. **1968**, *12*, 134.
(56) Feibelman, P. *J. Phys. Rev. B* **1995**, *51*, 17867.
(57) Fiorentini, V.; Methfessel, M.; Scheffler, M. *Phys. Rev. Lett*. **1993**, *71*, 1051.
(58) Leiva, E. P. M.; Del Popolo, M. G.; Schmickler, W. *Chem. Phys. Lett.* **2000**, *320*, 393.
(59) Cammarata, R. C. *Prog. Surf. Sci*. **1994**, *46*, p 1.